ENTAC 2024
XX ENCONTRO NACIONAL DE TECNOLOGIA DO AMBIENTE CONSTRUÍDO
Maceió, Brasil, 9 a 11 de outubro de 2024

# Calibration of a computer simulation with a test cell composed with a wall thermosyphons

## Calibração de uma simulação computacional com uma célula-teste composta com parede de termossifão

**Fernando da Silva Almeida**
Universidade Federal de Santa Catarina | Florianópolis | Brasil | fernando.almeida@labtucal.ufsc.br
**Rafael Roque Rossi**
Universidade Federal de Santa Catarina | Florianópolis | Brasil | rafael.roquerossi@gmail.com
**Marcia Barbosa Henriques Mantelli**
Universidade Federal de Santa Catarina | Florianópolis | Brasil | marcia@labtucal.ufsc.br
**Martin Ordenes Mizgier**
Universidade Federal de Santa Catarina | Florianópolis | Brasil | martin.ordenes@ufsc.br

**Abstract**

*Energy consumption is increasing exponentially. Studies indicate that the construction sector is one of the main contributors to such demands, and a significant portion of this consumption is dedicated to maintaining internal thermal comfort. Research indicates that irreversible global warming is underway until the end of this century. This emphasizes the dependence on mechanical climate control systems. In this context, passive cooling methods should be investigated. Thus, to broaden the investigation of these systems, the aim of this work is to calibrate a computational model, developed in the EnergyPlus software, with a test cell composed of a wall thermosyphon for internal cooling. The results from the first hour of IC and the last hour of Transient Condition were the ones that deviated the most from the calculated root mean square error limit for all simulated tests. These differences may be influenced by various factors, such as air infiltration into the test cell, system startup time, or even the thermophysical values of the materials used in the test cell envelope. In general, the data obtained in EnergyPlus were considered statistically equivalent to the experimental samples collected in the test cell, indicating, even with the use of simplifications, a coherent modelling with the experimental study.*

*Keywords: Calibration. EnergyPlus. Wall thermosyphons. Test cell.*

**Resumo**

O consumo de energia está aumentando exponencialmente. Estudos indicam que o setor da construção é um dos principais contribuintes para tais demandas, e uma parte significativa

Como citar:
ALMEIDA, F. S. et al. Calibration of a computer simulation with a test cell composed with a wall thermosyphons. In: ENCONTRO NACIONAL DE TECNOLOGIA DO AMBIENTE CONSTRUÍDO, 20., 2024, Maceió. **Anais**... Maceió: ANTAC, 2024.

desse consumo é dedicada à manutenção do conforto térmico interno. Pesquisas indicam que o aquecimento global irreversível está em curso até o final deste século. Isso enfatiza a dependência dos sistemas mecânicos de controle climático. Neste contexto, métodos de resfriamento passivo devem ser investigados. Assim, para ampliar a investigação desses sistemas, o objetivo deste trabalho é calibrar um modelo computacional, desenvolvido no software EnergyPlus, com uma célula-teste composta por um termossifão de parede para resfriamento interno. Os resultados da primeira hora de IC (Condição Inicial) e da última hora de Condição Transiente foram os que mais se desviaram do limite de erro quadrático médio calculado para todos os testes simulados. Essas diferenças podem ser influenciadas por diversos fatores, como infiltração de ar na célula-teste, tempo de inicialização do sistema ou até mesmo os valores termofísicos dos materiais usados no envelope da célula-teste. Em geral, os dados obtidos no EnergyPlus foram considerados estatisticamente equivalentes às amostras experimentais coletadas na célula-teste, indicando, mesmo com o uso de simplificações, uma modelagem coerente com o estudo experimental.

Palavras-chave: Calibração. EnergyPlus. Termossifões de paredes. Célula-teste.

## INTRODUCTION

Currently, energy consumption is increasing exponentially. Studies indicate that the construction sector is one of the main contributors to such demands [1]. In general, a significant portion of the energy consumed by buildings is dedicated to maintaining internal thermal comfort [2]. This highlights a dependence on climate control systems, which increase energy consumption in buildings [3]. Therefore, researching new passive solutions that reduce the energy requirement for user comfort becomes necessary [4].

Heat pipes and two-phase thermosyphons are high efficient heat transport passive solutions. These devices transfer heat without the need for additional energy consumption, even when subjected to small temperature differences, driven by imposed heat inputs and/or temperature levels at the evaporator and condenser regions [5].

In general, two-phase thermosyphons (Figure 1) are typically composed of an evacuated tube partially filled with a working fluid. They generally consist of three main parts: the evaporator, adiabatic section, and condenser. The evaporator is usually positioned below the condenser to allow the condensed fluid to return from the condenser to the evaporator by gravity. Heat supplied to the evaporator causes vapor generation in this region, as the working fluid is in a saturated state. Due to the pressure difference between the evaporator and the condenser, the vapor, slightly pressurized in the evaporator, flows longitudinally, passing through the adiabatic section and reaching the condenser. Upon contact with the condenser, where heat is removed, the vapor releases latent heat and condenses, with gravity causing the return of the condensed fluid to the evaporator. The condensed liquid, returning to the evaporator, forms a thin film on the tube wall through gravity. As long as there is a temperature difference between the sections, the process of evaporation and condensation will occur cyclically [6].

**Figure 1: Gravity-assisted two-phase closed thermosiphon.**

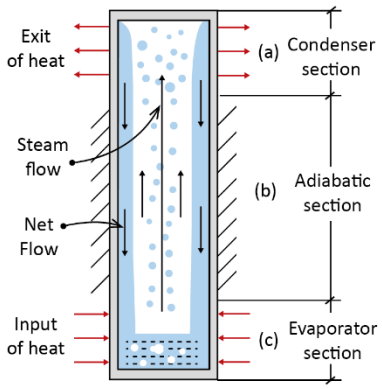


Source: Adapted [7].

This technology can be employed as solutions for thermal issues in various engineering applications, such as in baking and/or drying ovens; cooling units in the food industry; aircraft refrigeration, air conditioning, highway beds to prevent snow accumulation; in electronic components, heat exchangers and solar collector systems for energy generation [5]. Recently, the application of thermosyphons and heat pipes in the construction industry has been gaining prominence [8], [9], [10], [11], [12]. In this last application, thermosyphons are applied to walls of edifications to promote passive cooling of internal ambient by removing heat to the external environment. To design such systems, computational simulations can be a very useful tool.

Thus, the aim of this work is to calibrate a computational model, developed in the EnergyPlus software, to be used in the design of thermosyphon cooled walls in edifications, using data obtained from tests of a wood cell in which one of the walls was assisted by thermosyphons.

## METHOD

### EXPERIMENTAL SETUP: TEST CELL DESCRIPTION

The experimental evaluation was performed on a reduced-scale test cell, which simulated an internal ambient of a building. This is a usual strategy applied in the initial phases of many projects because these cells are cheaper to construct, more flexible regarding experimental arrangements and allows for different test dynamics. Besides, the instrumentation are easier to manage, resulting in better quality of collected data, among other factors [13].

The cubic test cell (Figure 2), had 60 cm of internal edge (each wall has a total area of 0.36 m²). The envelope of the cell consisted of three layers, with a total thickness of 80 mm. These layers were made of 15 mm thick MDF (Medium Density Fiberboard) sheets located on the external and internal faces of the model and filled with 50 mm thick polystyrene.

**Figure 2: Test cell.**

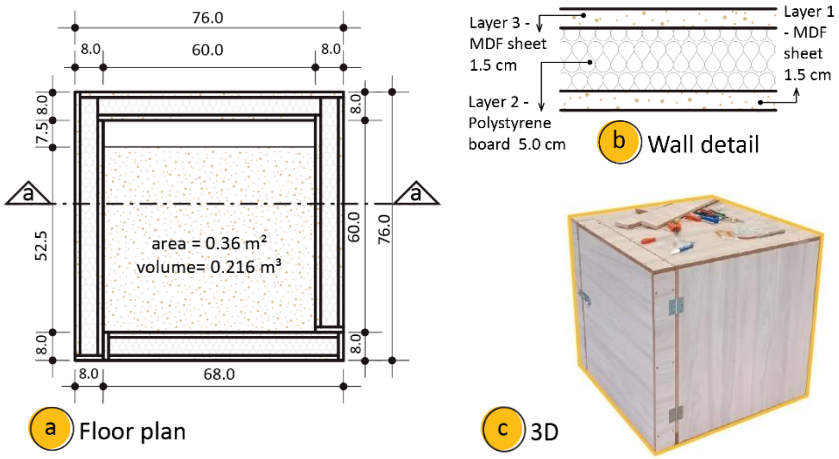


Source: The author.

In this experimental test, a copper coil was employed to simulate the thermal behaviour of the evaporator section of a two-phase loop thermosyphon. The temperature of the coil was maintained prescribed and uniform along its length by a controlled-temperature bath. The assembly has the shape of a coil (Figure 3) with a total length of 763.8 cm, consisting of copper tubes, 8 with a length of 78 cm and 2 with a length of 10 cm, both with an outer diameter of 22.22 mm (7/8) and a wall thickness of 0.79 mm (1/32). In addition, 16 copper curves with a 90° angle and the same diameter of the tubes were used to form the circuit. The tubes were joined to the curves and brazed. Finally, leak tests were performed.

**Figure 3: Copper Coil.**

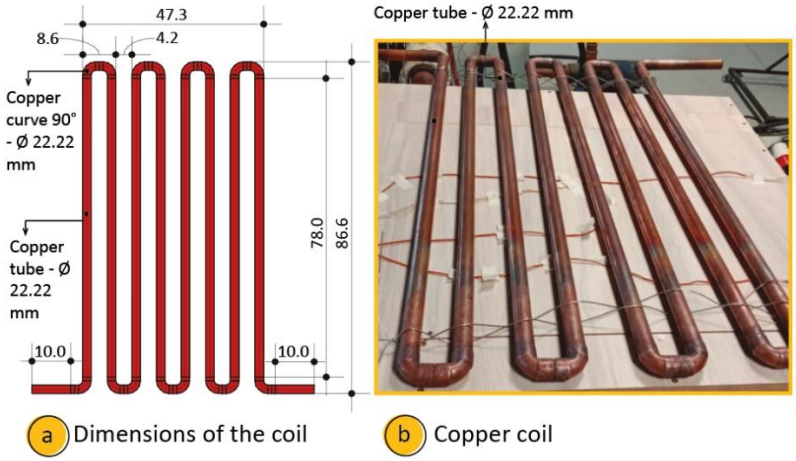


Source: The author.

After manufactured, the coil was coupled to the test cell. The copper coil was installed near the vertical wall behind the access door, which was referred as the Cold Surface (CS) in this work. To prevent unwanted thermal exchanges between the copper coil and the external environment, a ceramic fiber blanket was installed outside the test cell, thermally isolating the wall from the environment.

The temperatures of the test bench were measured using type K thermocouples, distributed in the central core of the cell. The 5-point method was used to distribute

the sensors in the core: one thermocouple is placed in the center and the others at four points in the diagonal line centers (see Figure 4a) [14], [15]. Thermocouples were also distributed along the coil, with two of them located at its inlet and outlet. The sensors were calibrated, resulting in an uncertainty of ±0.21 °C at a 95% confidence level.

**Figure 4: Distribution of thermocouples on the external, internal, and core surfaces of the test cell.**

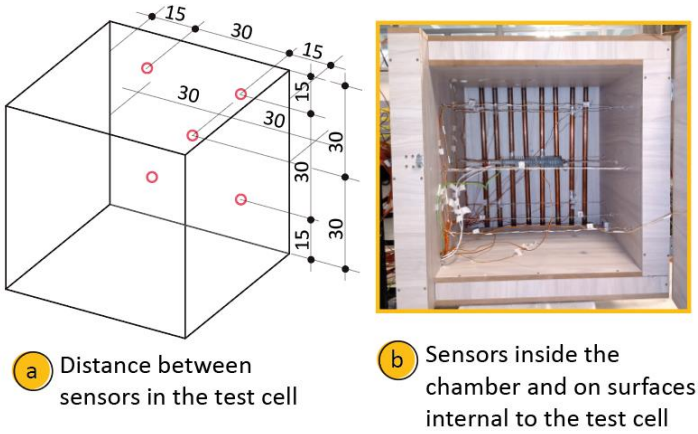


Source: The author.

A thermostatic bath was used to supply deionized water flow at a prescribed temperature that circulates inside the copper coil. The temperature-controlled thermostatic bath represented the operation of an evaporator section of a two-phase loop thermosyphon, which would absorb the heat generated in the internal ambient and transfer it out of the test cell, to be dissipated it into the external environment through its condenser, by, in this case, natural convection. To measure the volumetric flow rate of the cooling fluid, a high-precision rotameter was used. In this work, a flow rate of 2.06 l/min. was employed in all tests.

Heat was supplied to the core (internal ambient) of the test cell through electrical resistances located inside a finned aluminum heat sink, fed by a DC power supply, located at the center of the test cell. A data acquisition system was employed for data storage. Temperature readings were collected by the thermocouples every 30 seconds. To monitor the external air temperature around the test cell, a digital thermohygrometer recorder was used.

## EXPERIMENTAL PROCEDURE

The experiments were conducted in a laboratory, located on the 2nd floor, with the internal temperature controlled by air conditioning units, in levels close to 22°C. The laboratory is located in an urban area of the city of Florianópolis, Brazil (latitude -27.67, longitude -48.57, with an elevation of 6.1 m).

The following parameters were varied during tests: (1) the temperature of the water circulating through the copper coil, resulting in uniform distributed temperatures that simulates the evaporator conditions in an actual application, where the heat absorbed by the evaporator would be transferred to the thermosyphon's condenser, to be

removed to the environment; (2) the power dissipated by the electric resistance, which replicates thermal loads inside the cell. Two water temperatures were used: 22°C and 16°C. The internal thermal load was set at 25W and 20W. The combination of these variables resulted in 4 experimental tests (see Table 1).

**Tabela 1: Test parameters.**

| Test | Temperature of the thermostatic bath fluid (°C) | Power (W) |
|---|---|---|
| E1 | 22 | 25 |
| E2 | 16 | |
| E3 | 22 | 20 |
| E4 | 16 | |

Source: The author.

The tests occurred in two stages. In the first stage, heat electrical heater was turned on and the cell was let to achieve steady-state conditions, without the heat removal (by water in the coil), with the objective of establishing the initial conditions (IC), after which the ambient was cooled by the coil. Thus, for the first 15 hours, only the DC power supply remained on, transferring heat to the cell. Steady-state was considered achieved when the temperature variation was of 1% over a 30-minute interval. In the second stage, known as Transient Condition (TC), in addition to the heat source, the thermostatic bath was also activated, resulting in the circulation of water inside the copper tubes. Heat was removed from the inside test cell for 5 hours and steady-state conditions where again achieved, using the same temperature variation criterion. In total, each full cycle of tests lasted for 20 hours. More information about the experimental procedures can be found in XX et al. [16] work.

## CONSTRUCTION OF THE ENERGY BUILDING MODEL

Based on the characteristics of the laboratory (Zone 1) and the test cell (Zone 2), and considering the adopted experimental parameters, a numerical simulation was performed using EnergyPlus 23.1. Figure 5 shws the simulated volume, including the laboratory and the test cell. The climatic file was that of the Typical Meteorological Year (TMY, 2017-2021), for the city of Florianópolis, SC, Brazil. The inside and outside surface convention algorithms applied were TARP and DOE-2, respectively. Surface heat conduction was modelled using the Conduction Transfer Function [17].

**Figure 5: EnergyPlus simulation model.**

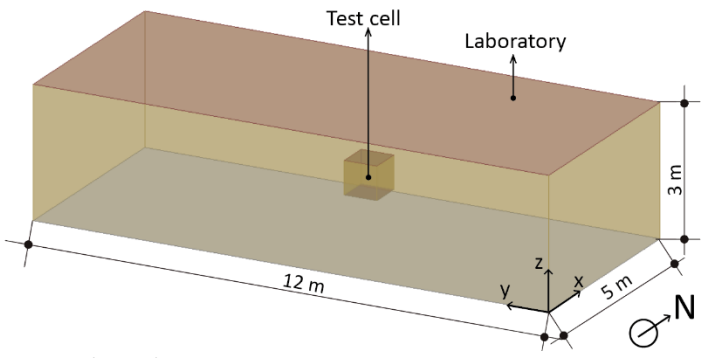


Source: The author.

The data considered for the laboratory and test cell walls are presented in Table 2. The walls on the north, south, and west sides, as well as the roof and floor of the laboratory, were modelled as adiabatic, since they were adjacent to other internal zones of the building. Concrete was considered for the floor and roof, while the walls were considered made of masonry blocks with an air gap, with a thermal resistance of 0.16 (m²K)/W, and external and internal finishes of mortar. On the other hand, the test cell was modelled as a zone within the laboratory, with different thermophysical properties assigned to the materials of its envelope (Table 2), as described in Section 2.1.

**Table 2 - Thermal properties of the materials used in the simulation model.**

| | Laboratory | | | Test Cell | | |
|---|---|---|---|---|---|---|
| | Floor and roof | Wall | | Seals | | Tube |
| Material | Concrete | Ceramic masonry block | Mortar | MDF | Polystyrene | Copper |
| Thickness (m) | 0.15 | 0.0134 | 0.025 | 0.015 | 0.05 | 0.00079 |
| Density (kg/m³) | 2300 | 1600 | 1800 | 720 | 52 | 8800 |
| Conductivity (W/mk) | 1.75 | 0.9 | 0.35 | 0.16 | 0.023 | 52 |
| Specific heat (J/kgK) | 1000 | 920 | 1000 | 1255 | 1210 | 420 |
| Absorbance (α) | 0.7 | 0.7 | 0.7 | 0.3 | 0.5 | 0.65 |

Source: The author.

The laboratory was modelled as a conditioned zone at 22°C, as in the experimental tests. Objects related to the “Ideal Load Air System” were used. For heat dissipation in the test cell, an electrical device with the same position of the electrical heater was considered, with the powers of 20w and 25W. Air infiltration from the environment to the test cell was modeled considering a flow rate of 0.00375 m³/s and a thermal velocity coefficient of 0,1.

The simulations were conducted following the same testing methodology adopted: the electrical equipment was turned on at 6:00 PM on Wednesday, providing heat until 2:00 PM on Thursday. Meanwhile, the system with constant water temperature was activated at 9:00 AM on Thursday, and it was turned off at 2:00 PM. It worths noting that the data from spring moths were considered, the same season in which the experiments were performed.

The constant-temperature water circulation system was modelled based on the basic example of a low-temperature constant-flow radiant system, provided by EnergyPlus, which considers the circulation of cold fluid through tubes embedded in a wall, ceiling, or floor and allows for electrical heating wires embedded in a surface or panel. In this context, the added energy is removed both by radiation heat exchange with the system and by convection of the surrounding air [18].

Table 3 presents the configuration the radiant system parameters used to simulate the controlled temperature thermal bath employed in the experiment.

**Table 3 - System configuration parameters.**

| Parameter | Vaçue |
|---|---|
| HVAC system type | Radiant chilled wall system with Daos |
| Thermal source presente after layer number | 3 |
| Temperature calculation requested after Layer number | 3 |
| Radiant pipes diameter | 22.22 mm |
| Radiant pipes spacing | 42 mm |
| Tube length | 4.8 m |
| Rated flow rate | $3.43x10^{-5}$ $m^3/s$ |
| Chiller parameter | Daos chiller autorized@ 2.5 and Radiant chiller autorized@ 2.75 |

Source: The author.

### THE ROOT MEAN SQUARE ERROR

A specific model is considered calibrated when they show statistically similar results [17]. To analyse the correspondence between measured and simulated air temperature data from the test cell, the root mean square errors (RMSE) were determined, using the following equation developed by Brown (2014) [19]:

$$\mathbf{RMSE} = \sqrt{\frac{\sum(\mathbf{x_i} - \mathbf{y_i})^2}{\mathbf{n}}} \quad (1)$$

where: n is the number of data points; yi is actual value of the ith data point; xi is the simulated value for the ith data point.

The lower the RMSE, the smaller the difference (error) between the simulated data in EnergyPlus and the test data.

### DATA TREATMENT

The data obtained from the experimental tests and simulations were processed using the software Excel, also used for generating images and tables. One parameter used for assessing the resemblance between measured and simulated data was the cooling rate Cr (°C/h), calculated from the expression:

$$\boldsymbol{C_r} = \frac{\Delta \boldsymbol{T}}{\boldsymbol{t}} = \frac{\boldsymbol{T_{CI}} - \boldsymbol{T_{CT}}}{\boldsymbol{t}} \quad (2)$$

where: ΔT is the difference between the average temperature of CI (TCI) and CT (TCT) in °C; t is the time of the test conducted in minutes.

## RESULTS

The comparison between simulation and experimental data are presented in this section. In Table 4, the RMSE values for the 4 tested trials are shown. The results of the average indoor air temperatures and cooling rates, for both measured and simulated results as a function of time, for time intervals of 1-hour, for tests in the cell subjected to power inputs of 20W and 25W (air heating) and coil temperatures of 22 and 16 °C, are illustrated in Figures 6, 7, 8, and 9. In these plots the first and last

temperatures of the Initial and Transient Condition ranges are also shown in rectangles.

In these figures, data related to the last 20 hours of tests are displayed, where the first 15 hours represent the Initial Condition (IC) and the last five hours the Transient Conditions (TC). The root mean square errors (RMSE) are also displayed in vertical bars over the simulated data (obtained through Equation 1). Cooling Rates were calculated using Equation 2 are plotted for the transient conditions.

In general, as observed in Table 4, a root mean square error lower than 0.50oC is noted for both conducted tests, which can be considered a low value. Actually, test E2 (16 °C - 25W) showed the lowest RMSE of 0.27 °C among all simulated cases.

**Table 4 - Results Root mean square error (RMSE).**

| Test | RMSE |
|---|---|
| E1 – 22 °C \| 25W | 0.48 °C |
| E2 – 16 °C \| 25W | 0.27 °C |
| E3 – 22 °C \| 20W | 0.41 °C |
| E4 – 16 °C \| 20W | 0.45 °C |

Source: The author.

In Figure 6 (E1 22 °C -25W), it is noticeable that during the Initial Condition, only in the first hour the experimental data was outside the RMS error around the simulated values, although they were quite close to each other. In the Transient Condition, a similar decaying exponential trend is observed in both data, but, however, the simulated value shows higher temperatures than experiments, which means that the extracted energy predicted was less than the measured value, resulting in lower cooling rates in four out of the five tested hours in the TC.

**Figure 6: Comparison of air temperature for measured and simulation results E1- 22 °C | 25W.**

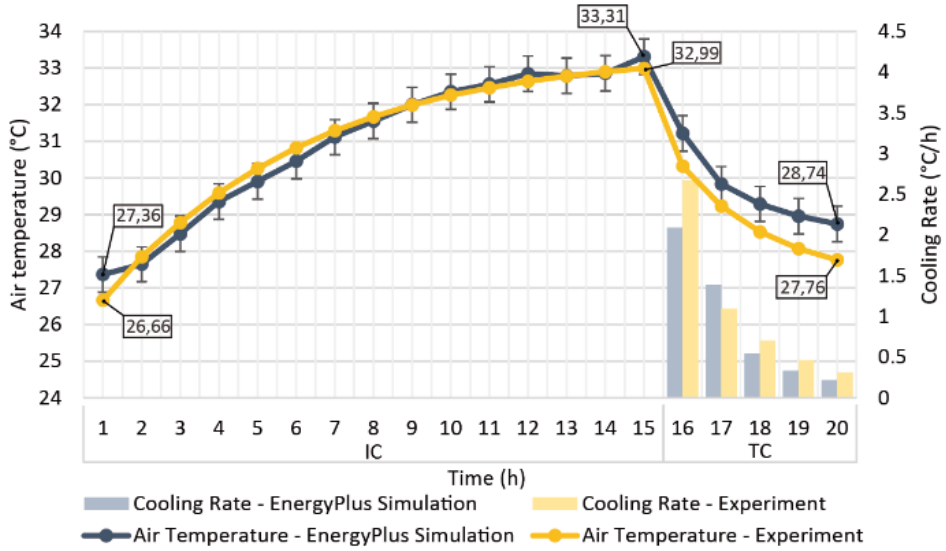


Source: The author.

As mentioned earlier, the simulated model E2 (16 °C - 25W), Figure 7, achieved the lowest error when compared to the other tests. Visually, it is possible to observe the similarity between the simulated and experimentally measured air temperatures. Similar to E1, the first hour in IC and the last hour in TC showed the greatest divergence

between the simulation and the experiment. In the last hour of TC, the simulation shows a stabilization of the results with the cooling rate tending to zero.

**Figure 7: Comparison of air temperature for measured and simulation results E2 -16 °C | 25W.**

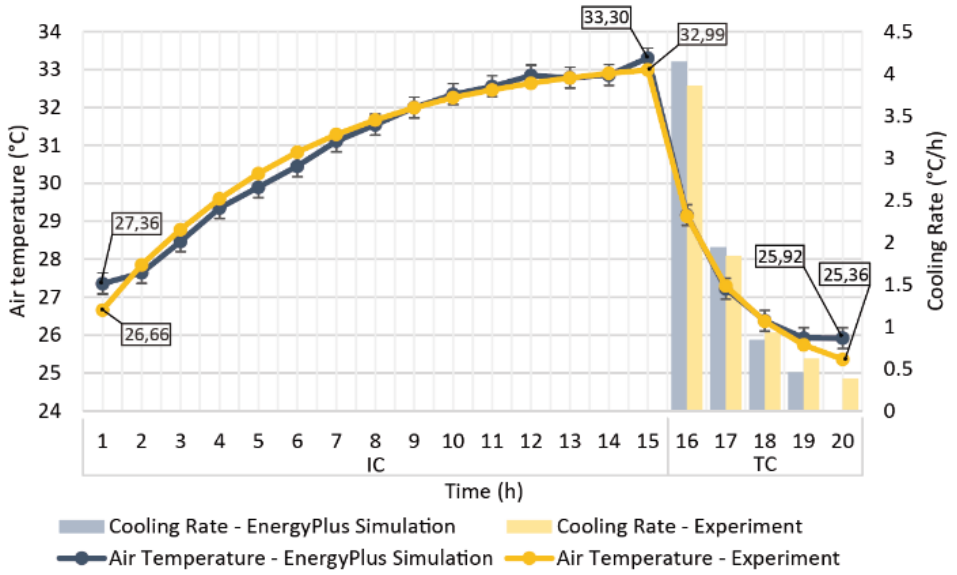


Source: The author.

In Figures 8 and 9, the results of tests E3 and E4 are presented, respectively. In both tests, the simulated model exhibited variation behaviours with temperature fluctuations higher than those shown by the experimental data during the Initial Condition. Between these two cases, E4 (16 °C - 20W) showed more curve similarity of experimental data with the simulations.

**Figure 8: Comparison of air temperature for measured and simulation results E3- 22 °C | 20W.**

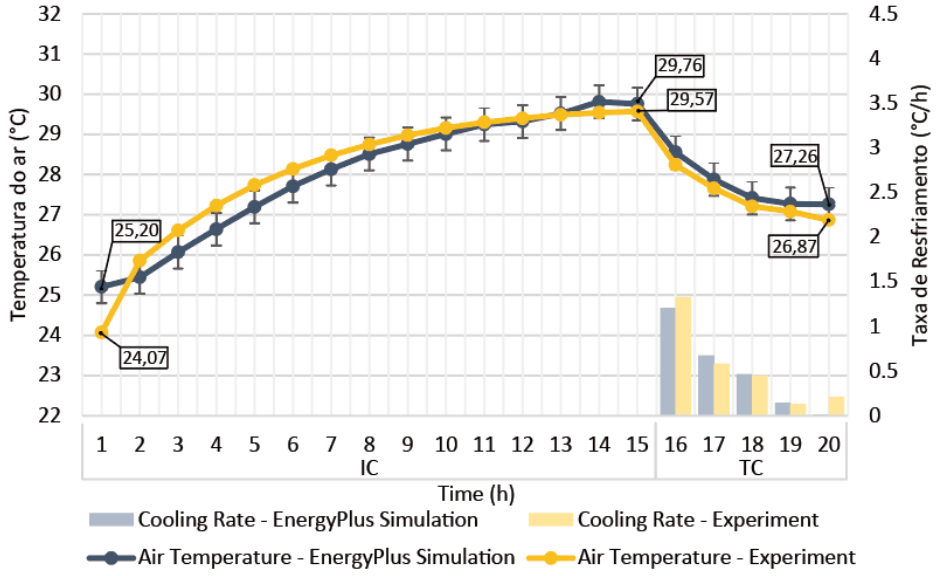


Source: The author.

**Figure 9: Comparison of air temperature for measured and simulation results E4- 16 °C | 20W.**

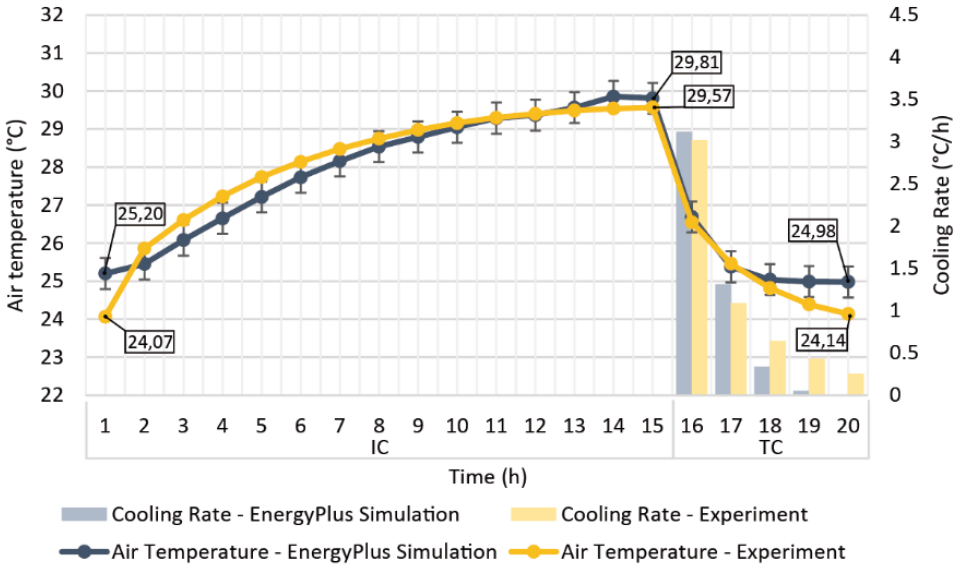


Source: The author.

In this sense, based on the results presented above, the comparisons between simulation model and experimental data were very satisfactory with RMSE lower than 0.5°C fir temperature levels of around 24 to 34°C, validating the simulation as a design tool for ambient cooled by the thermosyphons, where heat is removed from the internal ambient to external environment using two-phase thermosyphons.

## CONCLUSION

The indoor air temperature data of the test cell obtained using computational simulations were compared with the results from the experimental study with the objective of calibrating the simulation as a design tool. Similarities were observed between both the parameters used in the present study: the air temperature and the cooling rate. Both temperature curves showed similar behaviours.

However, as presented in section 3, the results from the first hour of IC and the last hour of TC were the ones that deviated the most (as observed by the curves) for all considered tests. These differences may be influenced by various factors, such as air infiltration into the test cell, system startup time, or even the thermophysical values of the materials used in the test cell envelope. In general, the data obtained in EnergyPlus were considered statistically equivalent to the experimental samples collected in the test cell, indicating, even with the use of simplifications, a coherent modelling of the observed physical phenomena.

Finally, the following subjects are proposed as future studies: (1) modelling the entire building where the laboratory is located, as the building's boundary conditions can influence the temperature results of the test cell; (2) a more in-depth evaluation of air infiltration into the test cell; and (3) measurement of the thermophysical properties of the materials used in the test cell for better simulated results quality.

## AGRADECIMENTOS

The authors thank the Institutional Program for Scientific and Technological Initiation (PIBIC/UFSC) and the Coordination for the Improvement of Higher Education Personnel (CAPES) for the financial support received for the development of this work.

## REFERÊNCIAS

[1] R. A. Betts, C. D. Jones, J. R. Knight, R. F. Keeling, and J. J. Kennedy, “Provisional State of the Global Climate 2023.” Sep. 2023. Accessed: Jan. 19, 2024. [Online]. Available: https://www.nature.com/articles/nclimate3063

[2] W. Athmani, L. Sriti, M. Dabaieh, and Z. Younsi, “The Potential of Using Passive Cooling Roof Techniques to Improve Thermal Performance and Energy Efficiency of Residential Buildings in Hot Arid Regions,” Buildings, vol. 13, no. 1, p. 21, Dec. 2022, doi: 10.3390/buildings13010021.

[3] D. G. L. Samuel, S. M. S. Nagendra, and M. P. Maiya, “Passive alternatives to mechanical air conditioning of building: A review,” Building and Environment, vol. 66, pp. 54–64, Aug. 2013, doi: 10.1016/j.buildenv.2013.04.016.

[4] C. Díaz-López, A. Serrano-Jiménez, K. Verichev, and Á. Barrios-Padura, “Passive cooling strategies to optimise sustainability and environmental ergonomics in Mediterranean schools based on a critical review,” Building and Environment, vol. 221, p. 109297, Aug. 2022, doi: 10.1016/j.buildenv.2022.109297.

[5] M. B. H. Mantelli, Thermosyphons and Heat Pipes: Theory and Applications. Cham: Springer International Publishing, 2021. doi: 10.1007/978-3-030-62773-7.

[6] Israa S. Ahmed and Ayad M. Al Jubori, “Assessment of heat transfer and flow characteristics of a two-phase closed thermosiphon,” Heat Transfer, doi: 10.1002/htj.21933.

[7] L. Zhou and C. Li, “Study on thermal and energy-saving performances of pipe-embedded wall utilizing low-grade energy,” Applied Thermal Engineering, vol. 176, p. 115477, Jul. 2020, doi: 10.1016/j.applthermaleng.2020.115477.

[8] Z. Zhang, Z. Sun, and C. Duan, “A new type of passive solar energy utilization technology-The wall implanted with heat pipes,” Energy & Buildings, vol. 84, p. 111, Dec. 2014, doi: 10.1016/j.enbuild.2014.08.016.

[9] F. Fantozzi et al., “An Innovative Enhanced Wall to Reduce the Energy Demand in Buildings,” J. Phys.: Conf. Ser., vol. 796, p. 012043, Jan. 2017, doi: 10.1088/1742-6596/796/1/012043.

[10] Z. Zhang and Z. Li, “Heat transfer performance of the Trombe wall implanted with heat pipes during daytime in winter,” Science and Technology for the Built Environment, vol. 25, no. 7, pp. 935–944, Aug. 2019, doi: 10.1080/23744731.2018.1538901.

[11] W. Yao, C. Liu, X. Kong, Z. Zhang, Y. Wang, and W. Gao, “A systematic review of heat pipe applications in buildings,” Journal of Building Engineering, vol. 76, 2023, doi: 10.1016/j.jobe.2023.107287.

[12] F. D. S. Almeida, M. P. Brandalise, L. H. Rodríguez, M. B. H. Mantelli, and M. O. Mizgier, “The potential of wall thermosiphon to reduce heat generated by internal charge density in residential bedrooms,” in BOOKS OF PROCEEDINGS, Santiago, Chile, 2022.

[13] G. Cattarin, F. Causone, A. Kindinis, and L. Pagliano, “Outdoor test cells for building envelope experimental characterisation – A literature review,” Renewable and Sustainable Energy Reviews, vol. 54, pp. 606–625, Feb. 2016, doi: 10.1016/j.rser.2015.10.012.

[14] L. Zhu, Y. Yang, S. Chen, and Y. Sun, “Thermal performances study on a façade-built-in two-phase thermosyphon loop for passive thermo-activated building system,” Energy Conversion and Management, vol. 199, p. 112059, Nov. 2019, doi: 10.1016/j.enconman.2019.112059.

[15] W. He et al., “Experimental study on the performance of a novel RC-PCM-wall,” Energy and Buildings, vol. 199, pp. 297–310, Sep. 2019, doi: 10.1016/j.enbuild.2019.07.001.

[16] F. D. S. Almeida, M. P. Brandalise, L. S. Fuso, L. H. R. Cisterna, M. B. H. Mantelli, and M. O. Mizgier, “Viabilidade da aplicação de termossifão bifásico para resfriamento passivo de ambientes internos,” PARC Pesq. em Arquit. e Constr., vol. 14, p. e023021, Sep. 2023, doi: 10.20396/parc.v14i00.8672200.
[17] P. Srivastava, Y. Khan, M. Bhandari, J. Mathur, and R. Pratap, “Calibrated simulation analysis for integration of evaporative cooling and radiant cooling system for different Indian climatic zones,” Journal of Building Engineering, vol. 19, pp. 561–572, Sep. 2018, doi: 10.1016/j.jobe.2018.05.024.
[18] Department of Energy, “EnergyPlusTM Version 23.1.0 Documentation - Engineering Reference.” 2023.
[19] N. Brown, S. Philip, I. S. Trojaola, S. Ubbelohde, and G. Loisos, “CALIBRATION OF AN ENERGYPLUS SIMULATION OF A PHASE CHANGE MATERIAL PRODUCT USING EXPERIMENTAL TEST CELL DATA,” 2014.